applied sciences

MDPI

Article

Easy Fabrication of Ultrafiltration Membrane via Polyethersulfone-Fumed Silica

Tutik Sriani [1], Budi Arifvianto [2], Ario Sunar Baskoro [3], Yudan Whulanza [3], Farazila Yusof [4,5], Gunawan Setia Prihandana [6,*] and Muslim Mahardika [2,*]

[1] Department of Research and Development, PT. Global Meditek Utama—IITOYA, Sardonoharjo, Ngaglik, Sleman, Yogyakarta 55581, Indonesia; tsriani@iitoya.com
[2] Department of Mechanical and Industrial Engineering, Faculty of Engineering, Universitas Gadjah Mada, Jalan Grafika No. 2, Yogyakarta 55281, Indonesia; budi.arif@ugm.ac.id
[3] Mechanical Engineering Department, Faculty of Engineering, Universitas Indonesia, Kampus UI, Depok 16425, West Java, Indonesia; ario@eng.ui.ac.id (A.S.B.); yudan@eng.ui.ac.id (Y.W.)
[4] Centre of Advanced Manufacturing & Material Processing (AMMP Centre), Department of Mechanical Engineering, Faculty of Engineering, Universiti Malaya, Kuala Lumpur 50603, Malaysia; farazila@um.edu.my
[5] Centre for Foundation Studies in Science, Universiti Malaya, Kuala Lumpur 50603, Malaysia
[6] Department of Industrial Engineering, Faculty of Advanced Technology and Multidiscipline, Universitas Airlangga, Jl. Dr. Ir. H. Soekarno, Surabaya 60115, Indonesia
* Correspondence: gunawan.prihandana@ftmm.unair.ac.id (G.S.P.); muslim_mahardika@ugm.ac.id (M.M.)

Abstract: This study investigated the effect of low-concentration fumed silica (FS) in polyethersulfone (PES) membranes. The PES/FS blend membrane was fabricated using a wet phase inversion technique as a flat sheet membrane. Scanning electron microscopy analysis revealed improved pore connectivity and rounder middle structures due to the addition of fumed silica. The experimental results indicated that the fabricated membranes fell within the ultrafiltration range, with pure water flux increasing as fumed silica concentration rose. The pure water flux improved by 64% compared to the native PES membrane. Furthermore, the blend membranes exhibited better selectivity, rejecting pepsin and lysozyme 11% and 19% more efficiently, respectively. Although the low concentration of fumed silica had minimal impact on the water contact angles of the membrane surface, all membranes demonstrated hydrophilicity. This cost-effective approach enhances permeability while maintaining separation characteristics, making it suitable for clean water applications.

Keywords: polysulfone; fumed silica; ultrafiltration; protein separation; clean water

Citation: Sriani, T.; Arifvianto, B.; Baskoro, A.S.; Whulanza, Y.; Yusof, F.; Prihandana, G.S.; Mahardika, M. Easy Fabrication of Ultrafiltration Membrane via Polyethersulfone-Fumed Silica. *Appl. Sci.* **2024**, *14*, 7290. https://doi.org/10.3390/app14167290

Academic Editor: Wenyi Wang

Received: 23 July 2024
Revised: 13 August 2024
Accepted: 15 August 2024
Published: 19 August 2024

1. Introduction

The current global water crisis is an urgent issue that requires immediate attention. The UN World Water Development Report 2020 highlights an imminent global water crisis resulting from water overuse, uncontrolled water contamination, and climate change. These factors contribute to clean water shortages, posing severe risks to livelihoods [1]. Surface water and groundwater contamination, especially in developing and Global South countries, poses challenges for people seeking access to clean water that meets WHO standards [2]. Water filtration plays a crucial role in removing impurities and contaminants from water using various media such as sand, charcoal, ion exchange media, distillation, and membrane filtration [3]. The growing concern over water scarcity and the need for easy clean water access have driven significant advancements in polymeric membranes for water and wastewater filtration [4].

Polyethersulfone (PES) is commonly employed for membrane application at different levels, from microfiltration to nanofiltration. This vast range of applications is partly attributed to its strong mechanical properties and chemical stability in acidic/alkaline states [5]. Despite these advantages, the hydrophobic characteristic of PES membranes makes them prone to fouling, which subsequently reduces water flux over time [6]. To

improve the anti-fouling properties of PES membranes, several additives have been investigated. Du et al. explored phospholipid biomimetic PES membranes by blending hydrophilic polymer and chloromethyl functional polyethersulfone [7]. While in vitro blood circulation confirmed its excellent anti-coagulant properties, its low protein retention did not meet the standards for hemodialysis membranes. Ahmad et al. studied the fouling behavior of mixed-matrix hollow fiber membranes PES/PVP/TiO_2 and observed an improved humic acid rejection compared to neat PES membranes, attributed to the higher surface hydrophilicity of TiO_2-blended membranes [8]. Another study integrated Ti_3AlC_2 MXene nanomaterials into a PES matrix to enhance membrane performance, demonstrating superior porosity and homogeneous pore size distribution due to the intrinsic properties of Ti_3AlC_2 [9]. Kallem et al. used hydroxyapatite to enhance the PES membranes' anti-fouling properties, with the negative charge groups on hydroxyapatite enhancing wettability and reducing irreversible fouling [10].

Silica stands out as a highly favorable inorganic additive owing to its low cost, ease of synthesis, and easy surface modification, hence enabling tailored properties for specific purposes. In the context of polymeric membranes, silica nanoparticles are often synthesized and incorporated into polymer structures as additives to achieve better performances. Researchers have explored functionalizing silica with various other materials into ultrafiltration membranes to enhance their performance, such as PVDF/Silica/Psf composite [11], zwitterionic functionalized silica nanogel [12], high-porosity silica sodalite [13], tetraethyl orthosilicate [14], and pyrazole-modified mesoporous silica [15]. Fumed silica nanoparticles are a promising membrane modifier candidate. Fumed silica is manufactured by the combustion of volatile silanes in an oxygen–hydrogen flame, hence offering a variety of fascinating properties, exhibiting a smooth and nonporous particle surface [16]. Mavukkandy et al. analyzed the impact of fumed silica particles as an inorganic additive on a polyvynilidenefluoride (PVDF) membrane, a microfiltration-range membrane, using dimethyl acetamide (DMAc) as a solvent. They revealed that while the PVDF-FS blend membrane exhibited significantly higher flux, it also had a high fouling tendency because its hydrophobicity increased [17]. Rutkevičius et al. synthesized non-fluorinated coatings for high-performance superhydrophobic coatings. They used a hybrid combination of fumed silica, polydimethylsiloxane, and polyurethane to develop an innovative, layered coating that demonstrated superhydrophobicity, robust abrasion resistance, and preferable air permeability [18]. According to their hypothesis, the extensive surface area and branched structure of fumed silica can be utilized to develop PDMS-PU and FS grafted coatings with improved functionalities. In their study, Samei et al. explored the permeation behavior of thin films composed of fumed silica-loaded polyvinyl alcohol (PVA) coated onto a tubular porous ceramic support. Using a solution-diffusion-based model that they developed, they revealed that the flux increased along with temperature and the loading of fumed silica, and decreased with the thickness of the membrane [19]. In the gas separation field, Isanejad and Mohammadi [20] investigated the modification of fumed silica nanoparticles with amine groups to develop a nanocomposite membrane. Their findings revealed that adding 15% of amine-functionalized fumed silica nanoparticles into the casting solution significantly improved the membrane's CO_2 permeability.

This study investigates the effects of incorporating a low concentration of fumed silica as a blend additive into a polyethersulfone casting solution for the fabrication of an ultrafiltration membrane. The goal was to enhance the membrane's selectivity properties while maintaining its permeability at ultrafiltration level. The membrane was prepared by the wet phase inversion technique. The effects of fumed silica at low concentrations on the surface morphology, pore parameters, water flux, and membrane hydrophilicity were investigated. The membrane's morphology was visually examined using scanning electron microscopy (SEM). To assess membrane performance and selectivity, the fabricated PES membranes were challenged with an aqueous solution containing proteins of varying molecular weights and the percentage of proteins retained by the membrane was calculated.

2. Materials and Methods

2.1. Materials

Polyethersulfone powder (PES, 62,000 g/mol, P.T. Solvay Chemicals, West Jakarta, Indonesia) was used as the polymer matrix. The solvent, NMethyl-2-Pyrrolidone (NMP), was sourced from Merck & Co., Inc., Kenilworth, NJ, USA. Fumed silica was acquired from Sigma Aldrich (St. Louis, MO, USA) with a molecular weight of 60.08 g/mol and surface area of 370–420 m^2/g. The fumed silica was acidic with a pH of 3.8–4.3 and a mesh residue of less than 0.02%. Additionally, bovine serum albumin (BSA), pepsin, and lysozyme were sourced from Himedia Laboratories Pvt. Ltd., Mumbai, India. Pure water was employed throughout the entire fabrication process. Unless otherwise specified, all chemicals were of analytical grade with a purity exceeding 98% and were used as supplied.

2.2. Membrane Preparation

Ultrafiltration membranes were prepared by non-solvent-induced phase separation (NIPS), a well-known process for creating various asymmetric membranes [21]. The casting solution was maintained at a constant 20 wt.% fraction of polyethersulfone. Initially, a solution containing PES and NMP was stirred at 70 °C until all polymers were completely dissolved. Subsequently, low concentrations of fumed silica particles were added as an additive. The PES solution was then mixed with 0.1 wt.% to 0.4 wt.% of fumed silica, heated, and stirred to create a uniform dope solution at 70 °C for 3 h. The dope solutions were then cooled down at room temperature for the further membrane-making process. After cooling, the dope solution was poured onto a glass plate and evenly casted using a film applicator (Elcometer, Manchester, UK) to achieve a uniform wet thickness of 150 microns. The glass plate containing the casted solution was then carefully transferred to a pure water bath to start the coagulation process. The membrane was soaked in pure water for 24 h before membrane testing. For clarity, the membranes were named based on their FS content: FS-0.0 (pure PES membrane), FS-0.1, FS-0.2, FS-0.3, and FS-0.4.

2.3. Membrane Characterization

In this study, the performance of the blend membranes was evaluated using pure water as the test fluid. The experiment was carried out for 30 min to achieve a stable flux in a stirred dead-end cell (HP4750 Stirred Cell, Sterlitech Corporation, Kent, WA, USA) with an effective membrane filtration area of 13.4 cm^2, as illustrated in Figure 1. To maintain consistent pressure in the pure water chamber, nitrogen gas was introduced into the dead-end-cell unit at a constant pressure of 2 bar. Throughout the experiment, the permeating water weight that penetrated through the tested membrane was recorded using a Weighing Environment Logger (A&D Co. Ltd., Tokyo, Japan). The equations below were utilized to determine the volumetric flux (J_v) and permeability flux (L_p) [22]:

$$J_v = \frac{Q}{A \times \Delta t} \tag{1}$$

$$L_p = \frac{J_v}{\Delta P} \tag{2}$$

where Q is the permeate water quantity during the sampling time, Δt is the sampling time, A is the area of the membrane, and ΔP is the pressure difference.

After conducting the water flux test, a membrane selectivity test was performed using a 1 g/L protein solution under identical conditions. For the protein separation test, three distinct protein types with concentrations of 0.1 wt% were used: bovine serum albumin (BSA, Mw = 66.5 kDa), pepsin (Mw = 40 kDa), and lysozyme (Mw = 14.3 kDa). These proteins were prepared in a phosphate-buffered solution with a pH of 7.2. The protein separation test was conducted using a dead-end cell filtration test, applying a fixed pressure of 2 bar. The concentration of proteins in the supernatant solutions, or the permeated liquid, were determined using a N4S UV-Visible Spectrophotometer (Ningbo Hinotek Instrument

Co., Ltd., Ningbo, China). The operational wavelength was set at 280 nm. This specific wavelength corresponds to the absorption peak of amino acids [23]. The solute rejection (SR) was determined by [24]:

$$\%SR = \left[1 - \frac{C_p}{C_f}\right] \times 100 \quad (3)$$

where C_p and C_f are the protein concentrations of the permeated and feed solutions, respectively. The data presented in this study represent the mean values of triplicate samples for each membrane.

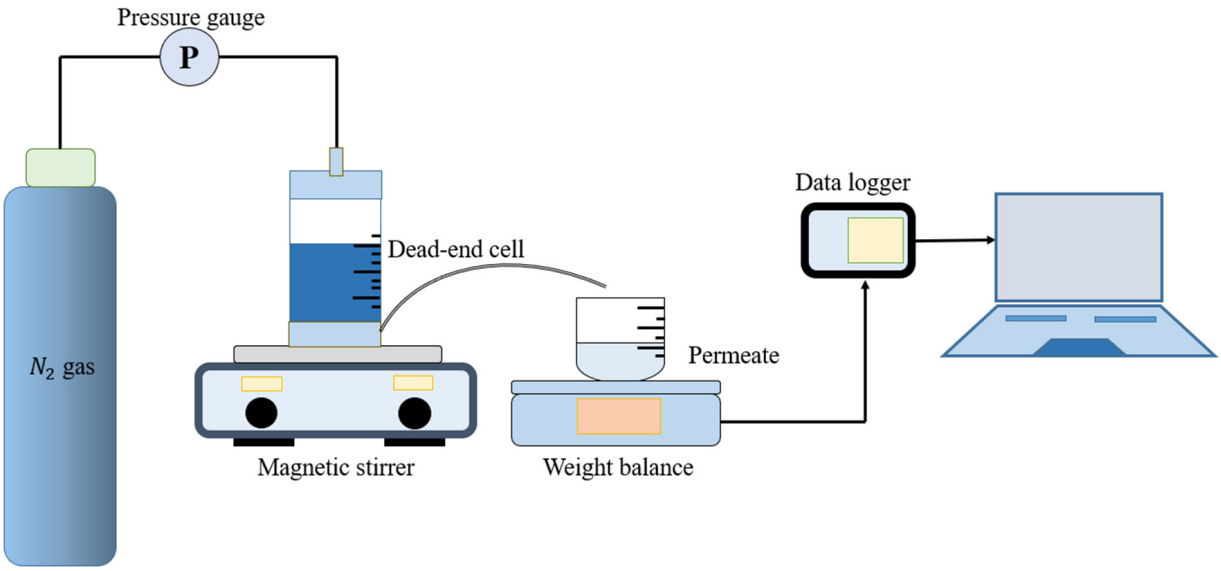

Figure 1. Configuration of the water flux test in a dead-end cell unit system.

The membrane's hydrophilicity was evaluated by measuring the contact angle between a water droplet and the membrane surface. A total of 5 µL pure water was carefully dropped on the surface of dried membrane using a micropipette. Subsequently, a digital microscope (Dino-Lite Edge 3.0 AM73915MZTL, Dino-Lite, New Taipei City, Taiwan), captured an image of the water's droplet contact angle. CAD software (AUTOCAD 2022) was used to measure the angle between the membrane and the droplet surface. To ensure precision, the contact angles were measured at four different locations, and the average value was calculated. The membrane surfaces and cross-sectional morphologies were examined using scanning electron microscopy (SEM Phenom ProX, Thermo Fischer, Waltham, MA, USA). Cross-section micrographs were acquired by fracturing the wet membrane samples after rapidly freezing them in liquid nitrogen.

2.4. Pore Characterization

To assess the membranes' surface porosity, the dry membranes were first cut to a specific size and subsequently immersed in glycerol for 1 day. The glycerol was carefully removed to acquire the wet membrane weight (W_w). The wet membrane was later placed in a desiccator and allowed to dry for 24 h to obtain the dry membrane weight (W_d). The membrane surface porosity was analyzed to assess the impact of incorporating fumed silica on membrane pore size. This analysis was conducted using a gravimetric method, which involves the following equation [25]:

$$\varepsilon(\%) = \frac{W_w - W_d}{\rho H_2O \times A \times L} \times 100 \quad (4)$$

where A is the effective area of the membrane, L is the thickness of the membrane, and ρH_2O is the density of the water. The average pore size (r_m) of the prepared membranes can be determined using the following the Guerout–Elford–Ferry Equation, based on the porosity and water flux data [26]:

$$r_m = \sqrt{\frac{(2.9 - 1.75\varepsilon)8\mu_{H_2O} \times L \times Q_{H_2O}}{\varepsilon \times A \times \Delta P}} \quad (5)$$

where ε is the membrane porosity, μ_{H_2O} is the dynamic viscosity of water at room temperature, L is the membrane thickness, Q_{H_2O} is the volume of water passing through the membrane per unit time, A is the active area of the membrane for filtration, and ΔP is the transmembrane pressure.

In ultrafiltration, the molecular weight cut-off (MWCO) is determined by filtering a range of molecules with known molecular weights, which are known to have a linear correlation with the size of the membrane pores [27]. According to a slit sieve model developed by Sarbolouki, the MWCO of a membrane is established by finding an inert solute with the smallest molecular weight that achieves at least 80% solute rejection during ultrafiltration experiments [28]. In this work, BSA (66.5 kDa), pepsin (40 kDa), and lysozyme (14.3 kDa) were selected for rejection studies using PES/FS blended membranes.

3. Results and Discussion

3.1. Membrane Morphology

Five membrane samples were prepared using varying fumed silica concentrations. Within this set of membranes, one membrane served as a reference without the addition of FS, denoted as FS-0.0. The other blend membranes were referred to as FS-0.1, FS-0.2, FS-0.3, and FS-0.4, corresponding to the FS weight concentration in the PES dope solution. All samples were cast with a wet thickness of 150 microns.

Figure 2 presents the SEM images of the cross-sections and top surfaces of the manufactured PES/FS membranes. The membranes have three distinct, asymmetric porous layers which comprise a dense spongy structure on the top surface, a finger-like porous sublayer in the middle, and a sparse spongy structure as the bottom layer. The three distinct layers can be explained as follows. The membrane was fabricated using a wet-phase inversion technique, where the dope solution changes phase from liquid to solid when immersed in pure water. During immersion, due to the exchange between NMP as solvent and pure water as non-solvent, precipitation occurs because the casted solution becomes thermodynamically unstable. In the surface, the casted solution is in direct contact with water and instantly vitrifies while allowing water to enter, generating microvoids. Hackett et al. explored the effect of coagulation bath composition on Psf membrane performance and stated that when only pure water was used during the immersion process, substantial residual solvent was entrapped in the middle part because of solvent–non-solvent incompatibility [29]. The hydrophilic nature of silica arises from the abundant silanol groups on its surface. Kang et al. [30] found that incorporating hydrophilic additives into the membrane dope solution enhances the exchange rate of solvent and non-solvent during the coagulation process. This, in turn, expands the size of the macrovoids at greater depth. When water infiltrates from the bottom, the coagulation rate differs from the top surface due to the presence of a glass support. As a result, this process leads to spongy structures similar to those on the top surface, but with larger pores. The results align with previous research findings reported elsewhere [31–33], including a ternary-phase field model simulation for a water/NMP/Psf system [21], which successfully predicts detailed asymmetric membrane structures comprised of a thick skin layer and a permeable sublayer.

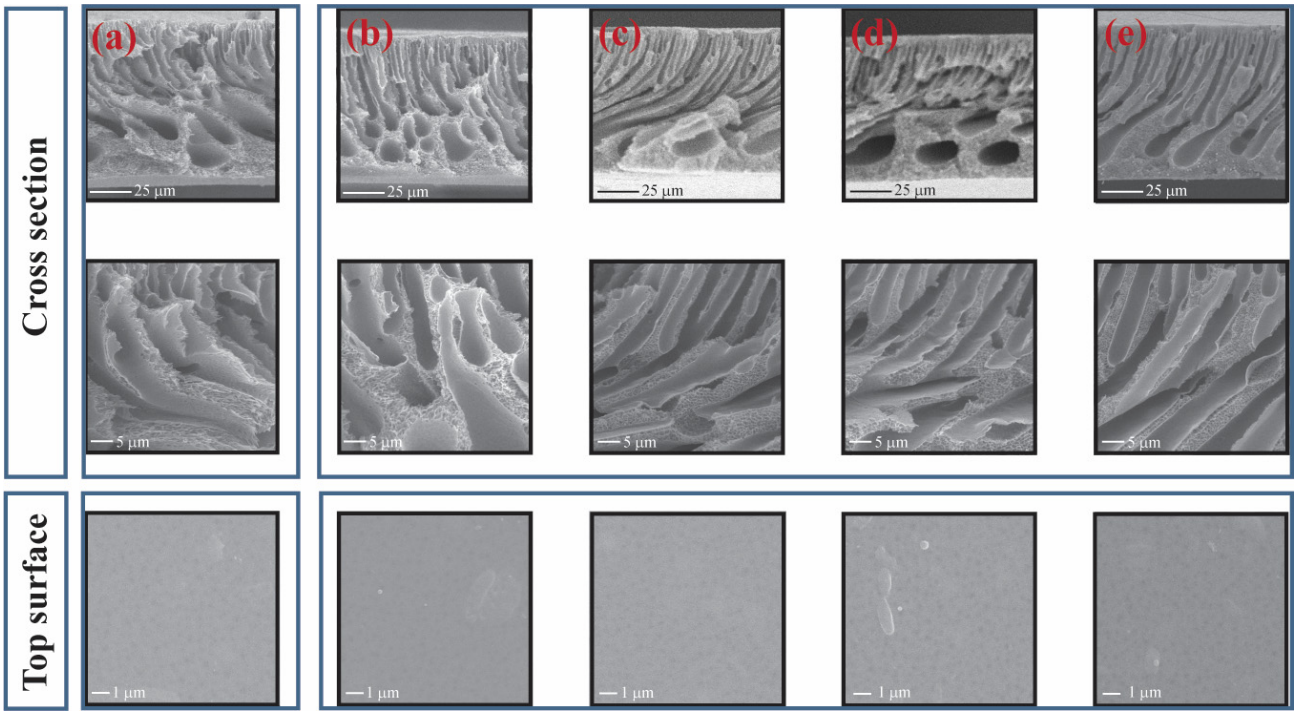

Figure 2. The morphologies of the blend membranes. Low and high magnification on the cross-section images is shown in the first and second rows. Top surface micrographs are shown in the third row: (**a**) FS-0.0, (**b**) FS-0.1, (**c**) FS-0.2, (**d**) FS-0.3, (**e**) FS-0.4.

As the fumed silica is introduced into the PES membrane, it induces more dark spots which are visible in the top surface micrograph. As the concentration of fumed silica increases, the quantity of these dark spots also increases. These dark spots correspond to voids within the membrane, which are indicative of open pores. The cross-section micrographs further confirmed that the addition of fumed silica leads to more open pores and the increased connectivity of the polymer wall. Additionally, membranes containing fumed silica exhibit a more organized structure compared to pure PES membrane, with rounder pore shapes. This may be because as the fumed silica content increased, the casting solution became thermodynamically less stable, resulting in an enhanced precipitation rate and the development of a more permeable membrane. The higher concentration of fumed silica disrupts the conglomeration of polymer molecules in the top layer during the coagulation process, resulting in a membrane with a more permeable top layer and potentially a more permeable sublayer [17].

3.2. Pure Water Flux Test Experiments

Figure 3 illustrates the pure water flux of PES/FS blend membranes in a dead-end filtration cell under a constant pressure of 2 bar. The pure water flux for the FS-0.0 membrane at this condition was 18.6 LMH/Bar. The value increased with FS concentration and reached the highest flux of 30.6 LMH/Bar when the membrane contained 0.3 wt.% fumed silica. This enhancement corresponded to a 64% improvement in flux. At concentrations beyond this point, the pure water flux declined to a level similar to that of the FS-0.2 membrane. This observation aligns with the research conducted by Mavukkandy et al., which investigated the effect of adding fumed silica to polyvynilidene fluoride (PVDF) membranes. They found that adding FS improved the membrane's permeability, showing a declining trend after reaching its optimum FS concentration [17]. Their analysis using ImageJ software further revealed that the increase in FS loading correlated with an enhancement in the membrane's surface porosity.

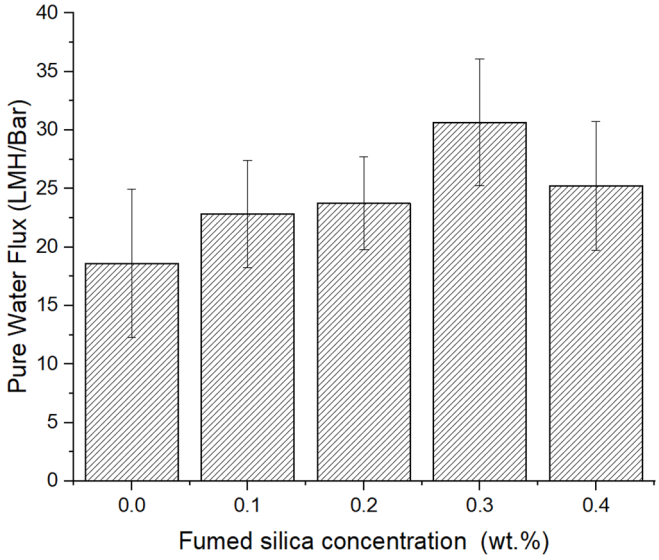

Figure 3. The pure water flux of PES membranes of varying fumed silica concentrations.

The water flux values improved substantially with a higher fraction of fumed silica. This enhancement can be attributed to improved interconnectivity within the membrane sublayer due to the presence of fumed silica. This observation aligns with the findings of Sen et al., who developed a composite membrane using spray-dried silica granules and polysulfone. Their study revealed that incorporating silica granules led to a twofold increase in flux compared to the native Psf membrane, which was due to additional pore channels generated by the spray-dried particles [34].

3.3. Protein Separation Performance Analysis

The level of protein adsorption on the membrane surface significantly impacts the measurement of fouling resistance ability. When protein adsorption is lower, the membrane exhibits greater resistance to fouling. This study investigated the impact of incorporating low-concentration fumed silica on polyethersulfone membranes for its selectivity and indicated the potential reduction in pore size that could occur with the introduction of fumed silica. The rejection rates for the aqueous solutions of proteins, including bovine serum albumin (66.5 kDa), pepsin (40 kDa), and lysozyme (14.3 kDa), were examined. Membranes selectively allow proteins of specific sizes to pass through. Smaller proteins can diffuse through larger pores, while larger proteins are retained. Figure 4 illustrates the protein rejection behavior of PES/FS membranes as a function of concentration. The selectivity of all membranes toward BSA was all above 90%, indicating a tight ultrafiltration membrane even without the addition of fumed silica. The FS-0.0 membrane has a rejection rate of 92%, while the other blends of PES/FS membranes reject an average of 95% BSA, indicating a close value to the reference. This implies that the pore size of a pure polyethersulfone membrane is sufficient to retain materials with molecular weights equal to or larger than BSA molecules, without the need to incorporate fumed silica into the dope solution.

Examining membrane rejection for smaller proteins, the PES/FS membranes outperformed the pure PES membrane. Specifically, for pepsin with a molecular weight of 40 kDa, the pure PES membrane exhibited a rejection rate of 76%, while the rejection rate for lysozyme was only 36%. Lysozyme is approximately 4.6 times smaller than BSA, and the rejection rate of the pure PES membrane already decreased by 56%. Conversely, the pepsin rejection rate for all PES/FS membranes is consistently above 83%, with FS-0.2 exhibiting the highest rejection rate of 87%, or an 11% improvement compared to the pure PES membrane. Moving on to the lysozyme, the smallest protein tested in this study, FS-0.2, also demonstrated the highest rejection rate of 55%. Interestingly, the trend of rejection is similar for both pepsin and lysozyme: it initially increases with the addition of fumed

silica up to 0.2 wt.%, but then decreases afterward. Figure 4 illustrates that PES membranes containing low concentrations of fumed silica perform well with molecules having a weight larger or at least close to 40 kDa. Maintaining the proper concentration of fumed silica was beneficial for salt rejection in desalination field; however, high FS content also led to membrane fouling [35]. The underlying mechanism involves a significant reduction in electrostatic repulsion between the fumed silica particles and the membrane surface, yielding stronger adhesion forces within the membrane regions [36].

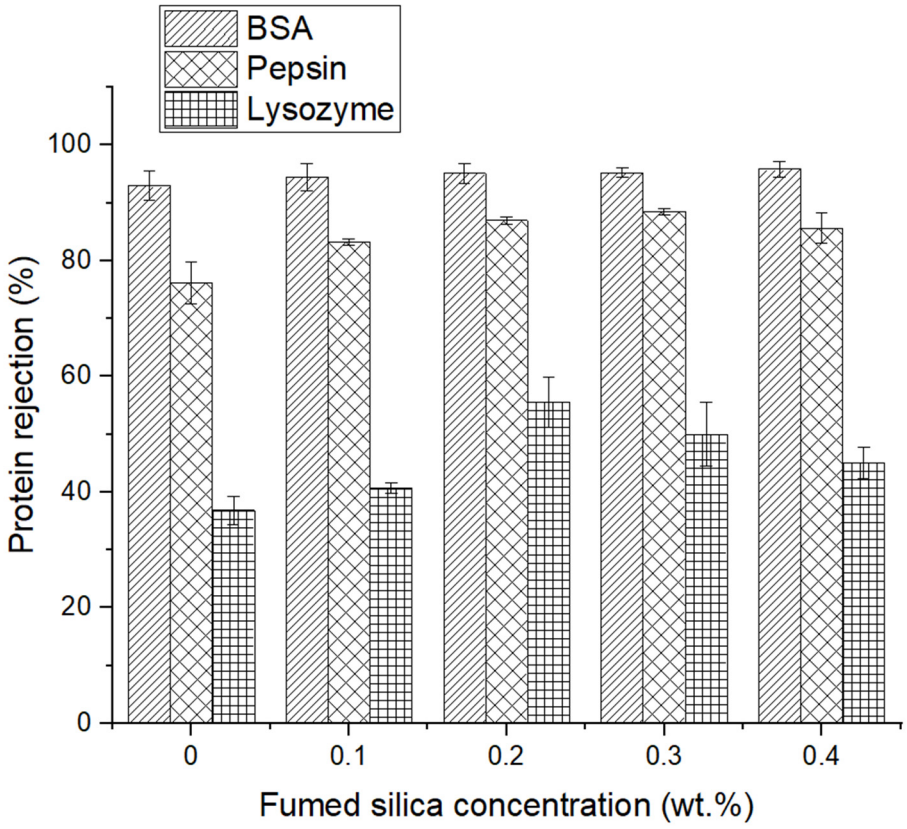

Figure 4. Protein rejection of PES membranes with varied fumed silica concentration.

3.4. Water Contact Angle Analysis

Water contact angle measurement is commonly employed to assess the hydrophilicity and wetting properties of membrane surfaces. Hydrophilicity behavior plays a crucial role in water treatment using membrane separation systems. The presence of silanol groups in fumed silica-added polymer membranes is likely to enhance membrane hydrophilicity, subsequently improving the permeation performance [37]. In this study, the water contact angle did not exhibit significant changes upon the addition of fumed silica, as illustrated in Figure 5. The native PES membrane has a contact angle of 60°, while the highest observed angle is 65°, with an average value of 63°. This lack of significant change may be attributed to the low concentration of fumed silica added, which is insufficient to significantly impact the surface water contact angle. Fumed silica is an amorphous material, and adding silica/fumed silica to a membrane solution normally increases its hydrophilicity because it contains a substantial amount of the hydrophilic silanol group [38]. According to Mavukkandy et al., the enhanced membrane hydrophilicity can be attributed to the FS residues within the polymer matrix, particularly on the membrane surface [17]. In this study, however, since the concentration of FS added to the PES solution was small, the increased hydrophobicity was not significant even though the trend was increasing.

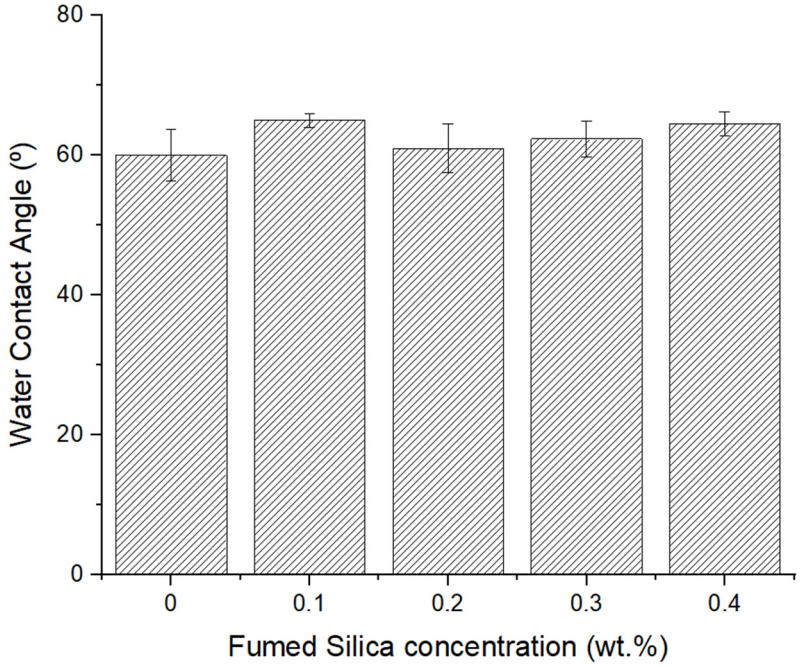

Figure 5. The water contact angle of PES membranes with varied fumed silica concentrations.

3.5. Pore Statistic Analysis

The surface porosity, mean pore size, and molecular weight cut-off are summarized in Table 1. Notably, it is interesting to observe from the table that incorporating low concentrations of fumed silica enhanced membrane porosity by up to 7.24% at FS-0.3. Simultaneously, the average pore size decreased with increasing fumed silica concentration, leading to a 13 kDa reduction in MWCO. The increased porosity suggests better pore distribution and improved interconnectivity, resulting in higher flux. This result aligns with the work of Lee and colleagues [39]. They developed mixed-matrix forward-osmosis (FO) membranes by combining silica gel with polyacrylonitrile (PAN) using a layer-by-layer assembly approach. This study revealed that the incorporated silica gel particles introduced additional pores within the membrane structure, which resulted in an increase in water flux during forward osmosis. Additionally, protein rejection improves as fumed silica concentration rises, indicating a smaller pore size, as supported by data in Table 1. However, rejection decreases subsequently, likely due to protein accumulation on the membrane pores.

Table 1. Pore statistics and MWCO of PES/FS blend membranes.

Membrane Code	Porosity, ε (%)	Mean Pore Size, r_m (Å)	MWCO, α (kDa)
FS-0.0	6.59	40.87	38
FS-0.1	6.95	30.02	25
FS-0.2	7.20	28.74	25
FS-0.3	7.24	28.25	25
FS-0.4	7.18	29.18	25

MWCO is a crucial parameter in filtration processes. It defines the size of solutes that can pass through a membrane, allowing them to selectively retain or remove specific molecules for various separation applications. In this work, when fumed silica was added, the decreased MWCO value enabled the retention of smaller molecules, which can then be utilized in diverse applications.

4. Conclusions

A polyethersulfone ultrafiltration membrane was modified with low-concentration fumed silica using a wet phase inversion method. The membrane's microscopic structure was analyzed using SEM. A key achievement in this work was enhancing water permeability without compromising separation characteristics. The PES/FS blend membranes containing 0.3 wt.% fumed silica exhibited the highest water flux, resulting in a 64% increase compared to the native PES membrane. All PES membranes demonstrated excellent BSA adsorption regardless of fumed silica addition. However, PES/FS blend membranes showed enhanced protein adsorption, with an 11% increase for pepsin and a 19% increase for lysozyme. Scanning electron microscopy images revealed better pore connectivity and a rounder middle structure in the blend membranes, contributing to improved permeability. As silica contains a silanol group which is naturally hydrophilic, the PES/FS blend membranes were expected to have increased hydrophilicity. However, since the concentration of fumed silica added was low, the water contact angles for all membranes remained very close. This cost-effective approach to enhancing permeability while maintaining separation characteristics could be scaled up for commercial applications.

Author Contributions: Conceptualization, G.S.P., M.M. and T.S.; methodology, T.S. and B.A.; software, T.S.; validation, Y.W., A.S.B. and M.M.; formal analysis, G.S.P.; investigation, G.S.P. and T.S.; resources, G.S.P., Y.W., A.S.B. and M.M.; data curation, T.S.; writing—original draft preparation, T.S.; writing—review and editing, T.S., Y.W., A.S.B., G.S.P., F.Y. and M.M.; visualization, T.S.; supervision, Y.W. and A.S.B.; project administration, M.M.; funding acquisition, G.S.P., Y.W., A.S.B., B.A., F.Y. and M.M. All authors have read and agreed to the published version of the manuscript.

Funding: This research and the APC were funded by Hibah Riset Kolaborasi Indonesia Scheme: Universitas Gadjah Mada (Grant No. 2692/UN1/DITLIT/Dit-Lit/PT.01.03/2023); Universitas Airlangga (Grant No. 958/UN3.LPPM/PT.01.03/2023); Universitas Indonesia (Grant No. NKB-1078/UN2.RST/HKP.05.00/2023).

Institutional Review Board Statement: Not applicable.

Informed Consent Statement: Not applicable.

Data Availability Statement: The original contributions presented in the study are included in the article, further inquiries can be directed to the corresponding author.

Acknowledgments: The authors would like to thank the staff of Universitas Gadjah Mada, Universitas Airlangga, and Universitas Indonesia for their administrative support.

Conflicts of Interest: The authors declare no conflicts of interest.

References

1. United Nations Educational, Scientific, and Cultural Organization. *United Nations World Water Development Report 2020: Water and Climate Change*; United Nations Educational, Scientific, and Cultural Organization: Paris, France, 2020.
2. Chen, Z.; Ngo, H.H.; Guo, W. A critical review on the end-uses of recycled water. *Crit. Rev. Environ. Sci. Technol.* **2013**, *43*, 1446–1516. [CrossRef]
3. Wang, X.; Chen, Y.; Fang, G.; Li, Z.; Liu, Y. The growing water crisis in Central Asia and the driving force behind it. *J. Clean. Prod.* **2022**, *378*, 134574. [CrossRef]
4. Hoslett, J.; Massara, T.M.; Malamis, S.; Ahmad, D.; Boogaert, I.V.D.; Katsou, E.; Ahmad, B.; Ghazal, H.; Simos, S.; Wrobel, L.; et al. Surface water filtration using granular media and membranes: A review. *Sci. Total Environ.* **2018**, *639*, 1268–1282. [CrossRef] [PubMed]
5. Esfahani, M.R.; Aktij, S.A.; Dabaghian, Z.; Firouzjaei, M.D.; Rahimpour, A.; Eke, J.; Escobar, I.C.; Abolhassani, M.; Greenlee, L.F.; Esfahani, A.R.; et al. Nanocomposite membranes for water separation and purification: Fabrication, modification, and applications. *Sep. Purif. Technol.* **2019**, *213*, 465–499. [CrossRef]
6. Otitoju, T.A.; Ahmad, A.L.; Ooi, B.S. Recent advances in hydrophilic modification and performance of polyethersulfone (PES) membrane via additive blending. *RSC Adv.* **2018**, *8*, 22710–22728. [CrossRef]
7. Du, Y.; Chen, X.; Mou, Y.; Chen, L.; Li, X.; Wang, J.; Shu, Y.; Zhao, Y.; Huang, N. Improving hemocompatibility and antifouling performance of polyethersulfone membrane by in situ incorporation of phosphorylcholine polymers. *Appl. Surf. Sci.* **2024**, *656*, 159646. [CrossRef]

8. Ahmad, A.L.; Pang, W.Y.; Shafie, Z.M.H.M.; Zaulkiflee, N.D. PES/PVP/TiO_2 matrix hollow fiber membrane with antifouling properties for humic acid removal. *J. Water Proc. Eng.* **2019**, *31*, 100827. [CrossRef]
9. Nabeeh, A.; Abdalla, O.; Rehman, A.; Ghouri, Z.K.; Wahab, A.A.; Mahmoud, K.; Abdalla, A. Ultrafiltration polyethersulfone-MXene mixed matrix membranes with enhanced air dehumidification and oil-water separation performance. *Sep. Purif. Technol.* **2024**, *346*, 127285. [CrossRef]
10. Kallem, P.; Bharath, G.; Rambabu, K.; Srinivasakannan, C.; Banat, F. Improved permeability and antifouling performance of polyethersulfone ultrafiltration membranes tailored by hydroxyapatite/boron nitride nanocomposites. *Chemosphere* **2021**, *268*, 129306. [CrossRef]
11. Song, H.J.; Kim, C.K. Fabrication and properties of ultrafiltration membranes composed of polysulfone and poly(1-vinylpyrrolidone) grafted silica nanoparticles. *J. Memb. Sci.* **2013**, *444*, 318–326. [CrossRef]
12. Li, X.; Nayak, K.; Stamm, M.; Tripathi, B.P. Zwitterionic silica nanogel-modified polysulfone nanoporous membrane by in-situ method for water treatment. *Chemosphere* **2021**, *280*, 130615. [CrossRef] [PubMed]
13. Eden, C.L.; Daramola, M.O. Evaluation of silica sodalite infused polysulfone mixed matrix membranes during H_2/CO_2 separation. *Mater. Today Proc.* **2021**, 38522–38527. [CrossRef]
14. Li, X.; Janke, A.; Formanek, P.; Fery, A.; Stamm, M.; Tripathy, B.P. High permeation and antifouling polysulfone ultrafiltration membranes with in situ synthesized silica nanoparticles. *Mater. Today Commun.* **2020**, *22*, 100784. [CrossRef]
15. Suhail, F.; Batool, M.; Anjum, T.; Shah, A.T.; Tabassum, S.; Khan, A.L.; AlMohamadi, H.; Najam, M.; Gilani, M.A. Enhanced CO_2 separation performance of polysulfone membranes via incorporation of pyrazole modified MCM-41 mesoporous silica as a nano-filler. *Fuel* **2023**, *350*, 128840. [CrossRef]
16. Barthel, H.; Rosch, L.; Weis, J. Fumed Silica—Production, Properties, and Applications. *Organosilicon Chem.* **1996**, *11*, 761–778.
17. Mavukkandy, M.O.; Bilad, M.R.; Kujawa, J.; Al-Gharabli, S.; Arafat, H.A. On the effect of fumed silica particles on the structure, properties and application of PVDF membranes. *Sep. Purif. Technol.* **2017**, *187*, 365–373. [CrossRef]
18. Rutkevičius, M.; Pirzada, T.; Geiger, M.; Khan, S.A. Creating superhydrophobic, abrasion-resistant and breathable coatings from water-borne polydimethylsiloxane-polyurethane Co-polymer and fumed silica. *J. Colloid Interface Sci.* **2021**, *596*, 479–492. [CrossRef]
19. Samei, M.; Iravaninia, M.; Mohammadi, T.; Asadi, A.A. Solution diffusion modeling of a composite PVA/fumed silica ceramic supported membrane. *Chem. Eng. Process.* **2016**, *109*, 11–19. [CrossRef]
20. Isanejad, M.; Mohammadi, T. Effect of amine modification on morphology and performance of poly(ether-block-amide)/fumed silica nanocomposite membranes for CO_2/CH_4 separation. *Mater. Chem. Phys.* **2018**, *205*, 303–314. [CrossRef]
21. Deng, X.; Yang, F.; Ma, J.; Li, Y.; Dang, J.; Ouyang, M. Ternary phase field model and characterization of water/NMP/polysulfone membrane prepared by non-solvent induced phase separation. *Sep. Purif. Technol.* **2024**, *330*, 125307. [CrossRef]
22. Saraswathi, M.S.S.A.; Rana, D.; Alwarappan, S.; Gowrishankar, S.; Kanimozhi, P.; Nagendran, A. Cellulose acetate ultrafiltration membranes customized with bio-inspired polydopamine coating and in situ immobilization of silver nanoparticles. *New J. Chem.* **2019**, *43*, 4216–4225. [CrossRef]
23. Kumar, M.; Lawler, J. Preparation and characterization of negatively charged organic-inorganic hybrid ultrafiltration membranes for protein separation. *Sep. Purif. Technol.* **2014**, *130*, 112–123. [CrossRef]
24. Kanagaraj, P.; Nagendran, A.; Rana, D.; Matsuura, T.; Neelakandan, S.; Malarvizhi, K. Effects of Polyvinylpyrrolidone on the permeation and fouling-resistance properties of Polyetherimide ultrafiltration membranes. *Ind. Eng. Chem. Res.* **2015**, *54*, 4832–4838. [CrossRef]
25. Manorma Ferreira, I.; Alves, P.; Gil, M.H.; Gando-Ferreira, L.M. Lignin separation from black liquor by mixed matrix polysulfone nanofiltration membrane filled with multiwalled carbon nanotubes. *Sep. Purif. Technol.* **2021**, *260*, 118231. [CrossRef]
26. Bagheripour, E.; Moghadassi, A.R.; Hosseini, S.M.; Ray, M.B.; Parvizian, F.; Van der Bruggen, B. Highly hydrophilic and antifouling nanofiltration membrane incorporated with water-dispersible composite activated carbon/chitosan nanoparticles. *Chem. Eng. Res. Des.* **2018**, *132*, 812–821. [CrossRef]
27. Rajagopalan, M.; Ramamoorthy, M.; Arthanareeswaran, G.; Raju, D.M. Cellulose acetate-poly(ether sulfone) blend ultrafiltration membranes. II. Application studies. *J. Appl. Polym. Sci.* **2004**, *92*, 3659–3665.
28. Sarbolouki, M.N. A general diagram for estimating pore size of ultrafiltration and reverse osmosis membranes. *Sep. Sci. Technol.* **1982**, *17*, 381–386. [CrossRef]
29. Hackett, C.; Hale, D.; Bair, B.; Manson-Endeboh, G.D.; Hao, X.; Qian, X.; Wickramasinghe, S.R.; Thompson, A. Polysulfone ultrafiltration membranes fabricated from green solvents: Significance of coagulation bath composition. *Sep. Purif. Technol* **2024**, *332*, 125752. [CrossRef]
30. Kang, Y.; Obaid, M.; Jang, J.; Ham, M.H.; Kim, I.S. Novel sulfonated graphene oxide incorporated polysulfone nanocomposute membranes for enhanced-performance in ultrafiltration process. *Chemosphere* **2018**, *207*, 581–589. [CrossRef]
31. Sadrzadeh, M.; Bhattacharjee, S. Rational design of phase inversion membranes by tailoring thermodynamics and kinetics of casting solution using polymer additives. *J. Memb. Sci.* **2013**, *441*, 31–44. [CrossRef]
32. Prihandana, G.S.; Maulana, S.S.; Soedirjo, R.S.; Tanujaya, V.; Pramesti, D.M.A.; Sriani, T.; Jamaludin, M.F.; Yusof, F.; Mahardika, M. Preparation and characterization of Polyethersulfone/activated carbon composite membranes for water filtration. *Membranes* **2023**, *13*, 906. [CrossRef] [PubMed]

33. Liu, G.; Zhang, L.; Mao, S.; Rohani, S.; Ching, C.; Lu, J. Zwitterionic chitosan-silica-PVA hybrid ultrafiltration membranes for protein separation. *Sep. Purif. Technol.* **2015**, *152*, 55–63. [CrossRef]
34. Sen, D.; Ghosh, A.K.; Mazumder, S.; Bindal, R.C.; Tewari, P.K. Novel polysulfone-spray-dried silica composite membrane for water purification: Preparation, characterization and performance evaluation. *Sep. Purif. Technol.* **2014**, *123*, 79–86. [CrossRef]
35. Sabir, A.; Islam, A.; Shafiq, M.; Shafeeq, A.; Butt, M.T.Z.; Ahmad, N.M.; Sanaullah, K.; Jamil, T. Novel polymer matrix composite membrane doped with fumed silica particles for reverse osmosis desalination. *Desalination* **2015**, *368*, 159–170. [CrossRef]
36. Bowen, W.R.; Doneva, T.A. Atomic force microscopy studies of membranes: Effect of surface roughness on double-layer interactions and particle adhesion. *J. Colloid Interface Sci.* **2000**, *229*, 544–549. [CrossRef] [PubMed]
37. Othman, M.H.D.; Hubadillah, S.K.; Adam, M.R.; Ismail, A.F.; Rahman, M.A.; Jaafar, J. Chapter 7—Silica-Based Hollow Fiber Membrane for Water Treatment. In *Current Trends and Future Developments on (Bio-) Membranes*; Elsevier: Amsterdam, The Netherlands, 2017; pp. 157–180. ISBN 9780444638663.
38. Liu, X.; Ng, H.Y. Fabrication of layered silica-polysulfone mixed matrix substrate membrane for enhancing performance of thin-film composite forward osmosis membrane. *J. Memb. Sci.* **2015**, *481*, 148–163. [CrossRef]
39. Lee, J.Y.; Qi, S.; Liu, X.; Li, Y.; Huo, F.; Tang, C.Y. Synthesis and characterization of silica gel–polyacrylonitrile mixed matrix forward osmosis membranes based on layer-by-layer assembly. *Sep. Purif. Technol.* **2014**, *124*, 207–216. [CrossRef]